Quaternary International xxx (xxxx) xxx

Contents lists available at ScienceDirect

Quaternary International

journal homepage: www.elsevier.com/locate/quaint

Holocene evolution of the Cávado estuary (NW Portugal)

Helena Granja [a,*], Luis Gómez-Orellana [b], Ana Luísa Costa [a], Rui Morais [c], César Oliveira [d], Pablo Ramil-Rego [b], José Luís Pinho [e]

[a] CIIMAR, Terminal de Cruzeiros do Porto de Leixões, Av. General Norton de Matos s/n, 4450-208, Porto, Portugal
[b] GI-1934 Territorio & Biodiversidade, IBADER, Universidade de Santiago de Compostela, Campus Terra s/n, 27002, Lugo, Spain
[c] FLUP/ID&CECH, Via Panorâmica, s/n, 4150-564, Porto, Portugal
[d] HERCULES Laboratory, University of Évora, Largo Marquês de Marialva, 8, 7000-809, Évora, Portugal
[e] Center of the Territory, Environment and Construction (CTAC), University of Minho, Campus de Gualtar, 4710-553, Braga, Portugal

ARTICLE INFO

Keywords:
Holocene
Cávado
Palaeoestuary
Sediments
Palaeobotany
Environments

ABSTRACT

This paper aims to contribute to the understanding of the Holocene evolution of the Cávado estuarine coastal system (Portugal) and the adjacent terrestrial areas, using a multidisciplinary approach, which includes geomorphology, sedimentology, palynology, radiocarbon and history. During the Early Holocene, the Cávado environment was characterized by the dominance of coarse sediments especially in the most westward areas, corresponding to fluvial energetic dynamics. During the Middle Holocene, the presence of wetlands dominated especially in the most sheltered areas. The pollen data reflect the predominance of forests during the initial phases of the introduction of agriculture, with a significant presence of humid forests. Between 4240 and 3980 cal BP, a sudden marine flooding took place over the peat. During the Late Holocene, there was a succession of low, high and again low energy fluvial environments in the eastward sheltered areas, while high energy dominated in the Fão channel entrance, with marine influence on the uppermost units. The pollen content reflects a situation of high human influence, with a poor representation of natural forests and a predominance of agrosystems, related to the rise of the Cávado estuary as a port during the heyday of the city of Braga during the Roman and Suevian periods, as described in historical texts and archaeological research. In connection with this growth, the pollen data show the existence of local Pinus plantations related to shipbuilding and repair in the port. During these times, the estuary was larger and open to the sea at Fão. After the 15th century, with the general silting of coastal areas, the inlet closed and the river mouth was displaced to the North.

1. Introduction

An estuary, being a semi-enclosed, coastal body of water, which has free connection with the open sea and within which sea water is measurably diluted with fresh water derived from land drainage (Pritchard, 1952). It is a particular environment subject to rapid changes in sedimentary budgets forced by different ocean and terrestrial control factors. During the Holocene, the most important factors controlling the infilling of river palaeovalleys in non-glaciated terrains included eustatic sea level rise, continental erosion, availability of shelf sediment, and local hydrodynamics (Boski et al., 2008) and neotectonics (Granja, 1999; Granja et al., 2010). Sedimentary budget is dependent on climate, vegetation cover, land use changes and adjustments in the hydrographic basin, being a natural archive of processes which occurred during the Holocene, including indicators of quick events such as floods, storm surges and tsunamis (Ramos-Pereira et al., 2019). They also offer indications of regional and/or local climatic changes, reflected in the land cover, hydrography and availability of sediments.

During a rapid sea level rise, open marine embayments convert into lagoons and estuaries protected by clastic barriers. Barrier onset and initiation of deposition inside the lagoons took place between 8000 and 5300 cal BP in NW Iberia, according to González-Villanueva et al. (2015).

The palaeoenvironmental reconstruction of the NW coastal zone of Portugal during the Late Holocene pointed to a segmented barrier coast with confined freshwater or slightly brackish lagoons between small headlands, in depressed areas of the rocky shore platform, whose barriers would be located westwards of the contemporary coastline (when present beaches lose sand it is possible to observe Holocene silty-clayey deposits extending below low tide). These aquatic environments were

* Corresponding author.
E-mail address: hgranja@dct.uminho.pt (H. Granja).

https://doi.org/10.1016/j.quaint.2022.02.032
Received 13 April 2021; Received in revised form 11 February 2022; Accepted 28 February 2022

subject to progressive silting until their disappearance. Some of the wetlands around the Cávado river were still active at the beginning of the 20th century (Viana, 1928) and the Apúlia lagoon (Fig. 1) is still in a peat building late phase (Granja et al., 2010).

The morphology and position of the lower reach of the Cávado river, crossing the rocky shore platforms, has changed over time. One question this paper is concerned with is the position of the former inlet and the morpho-sedimentary conditions of the lower Cávado. Historical and archaeological data indicate the presence of an inlet southward of the present inlet, at Fam (present Fão) at least from the 12th to the 16th century. Several royal and church sources refer to the importance of salt exploitation at Fão, which means that interchanges with the ocean were present at the time.

This paper is an attempt to clarify the historical and archaeological data regarding the Cávado river mouth and the adjacent coastal areas as well as to improve the output of the previous NAVANCOR (2013–2015) project and other research on the Cávado (e.g. Granja, 1999; Granja et al., 2010; Ribeiro and Granja, 2000). Three new percussion cores have been taken in order to obtain more complete data to aid in understanding the Holocene palaeoenvironmental evolution of the zone (Fig. 1). The cores were located at Barqueiros (core NAV1) and at Bonança (cores NAV4 and NAV5). The location of NAV1 was chosen based on important data concerning Cávado evolution obtained from a previous core in the area (Granja, 1999); NAV4 and NAV5 were selected according to the presumed historical location of the old Cávado inlet (Fam inlet). The pollen data allow for the clarification of the influence of historical events on the environment in a period of great importance, which includes the foundation and rise of the city of Braga and its relationship with the sea through the Cávado River. Along the Esposende coast, the existence of a huge quantity of artefacts, especially amphorae, point to natural anchorage conditions important for Atlantic trade in the 1st BC and 1st AD millennia (Almeida, 2005; Granja and Morais, 2012; Morais, 2013).

2. Geological and geomorphological background

The bedrock of the Cávado estuary and nearby coastal zone consists of two Palaeozoic formations - Ordovician and Silurian - and granites, crossed by quartz veins (Teixeira et al., 1969). Both formations constitute a syncline with a NW–SE axis. The eastern flank is in contact with the granites through NW–SE faults and shear zones. The western flank is offshore and submerged for the main part, the Ordovician rocks constituting the outcrops of present beaches. The Plio-Pleistocene sediments rest over the top of the rocks forming the syncline (Fig. 1).

The orientation of the shoreline is controlled by fault strikes (NW–SE, NE–SW and E–W) crossing the syncline. Some of these faults were reactivated during the Pleistocene–Holocene (Cabral, 1993) and neotectonic indicators are present (Granja, 1999).

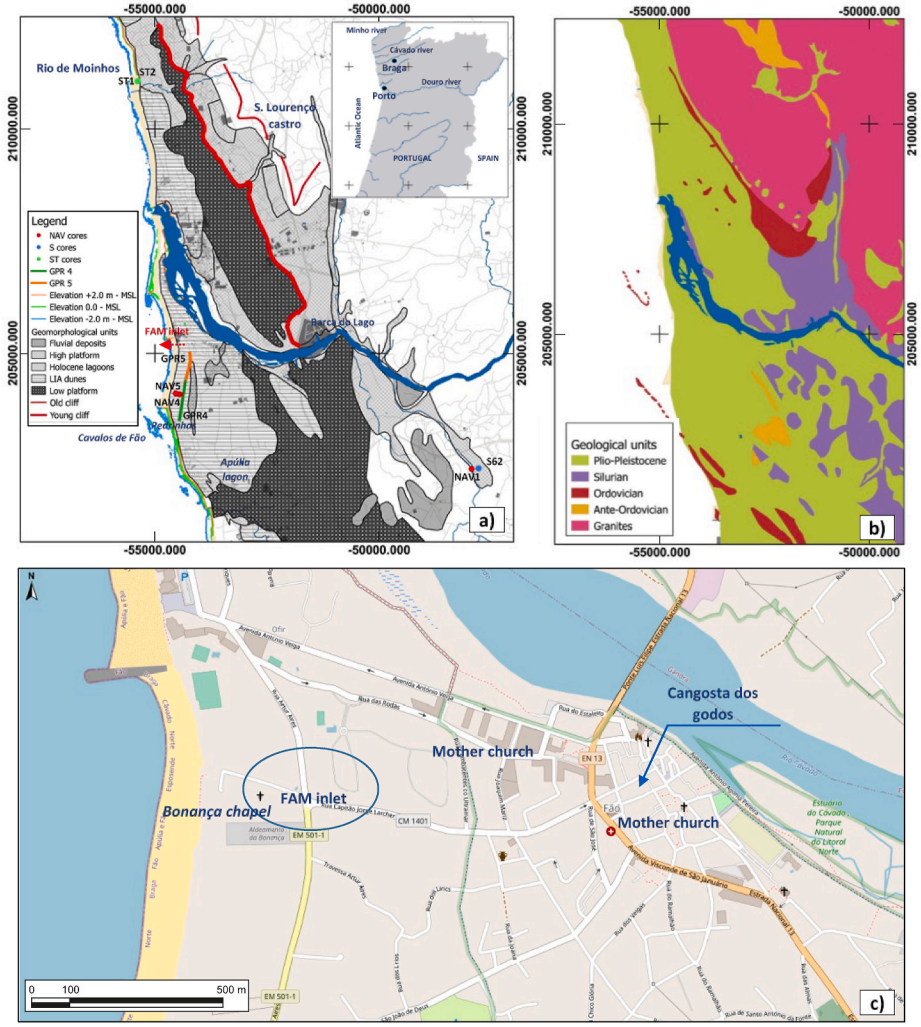

Fig. 1. Study area (41°30′30′′N; 8°46′57′′W). A: main geomorphological units with core positions; B: simplified geological map; C: location of GPR profiles and places cited in text.
Coordinates: Datum ETRS89 Portugal TM06.

The Cávado river is the boundary between two structural compartments with different morphology and sedimentary distribution (Fig. 1). The geomorphology is characterized by two main shore platforms (narrowing from South to North), one at a mean height of 50–60 m MSL and the other from 30 m MSL extending on a smooth slope below sea level, separated by a small cliff. A dead cliff of uncertain age in granite, about 200 m MSL, is the landward limit of this coastal zone. Due to a slight dip to the N of the shore platforms and to neotectonics, Holocene sediments and Little Ice Age (LIA) dunes are more abundant in the northern compartment than in the southern compartment, where they are residual and Pleistocene sediments extend inland at a higher position in the absence of the dead cliff (Granja, 1999).

3. Methods

3.1. Cores

The sedimentary sequence above bedrock was obtained with a percussion corer, in an agricultural field at point NAV1, located at Barqueiros, 41°29′19.5'' N and 8°42′27.1'' W, 363 cm MSL (Fig. 1). NAV4, 41°30′18.50" N and 8°47′3.92" W, 213 cm MSL and NAV5, 41°30′19.12" N and 8°47′7.52" W, 325 cm MSL, were drilled by way of the same process as at Bonança, in an area of LIA dunes, at the back of present beaches (Fig. 1). Cores were split in two halves, one for macroscopic facies description and sampling for further analyses (sedimentology, palynology and dating), and the other for archive.

Table 1
Radiocarbon datings, $^{13}\delta$, depth (cm), MSL elevations (cm), sedimentation rates (mm/yr), and type of sediment of dated samples. In bold, the range with the highest probability is indicated and in parentheses the relative area under probability distribution.

Core	Sample	Lab. Ref.	Material	Depth (cm)	Height MSL (cm)	^{14}C BP conventional	δ^{13}C	Cal BP (2 σ)	Cal BC/AD (2 σ)	Sedimentation rates (mm/yr)
NAV1	NAV1.93	Beta-400091	organic sediment	72	+291	1010 ± 30	- 26.0	798-813, 816–869, **901–958(0.735)**	Cal AD **992–1049 (0.735)**,1081–1134, 1137-1152	2.34 1.00 0.71
NAV1	NAV1.79	ICA-18OS/0842	organic sediment	168	+195	1450 ± 30	–	**1299–1379(1)**	**Cal AD 571–651(1)**	0.44 0.35
NAV1	NAV1.58	Beta-400089	organic sediment	356	+7	3030 ± 30	- 24.6	3083-3089, 3115–3118, **3148–3277(0.686)**, 3280-3348	Cal BC 1399–1331, **1328–1199(0.686)**, 1169–1166, 1140-1134	
NAV1	NAV1.46	ICA-20P/0614	peat	420	- 57	3750 ± 30	- 27.62	3986-4049, **4064–4159(0.630)**, 4168-4182, 4199-4232	Cal BC 2283–2250, 2233–2219, **2210–2115 (0.630)**, 2100-2037	
NAV1	NAV1.23	ICA-20P/0613	peat	540	- 177	5990 ± 40	- 26.14	**6733–6945(1)**	Cal BC **4996–4784(1)**	
NAV1	NAV1.8	Beta-400090	organic sediment	645	- 282	8810 ± 40	- 26.1	**9680–9963(0.815)**, 9986–10015, 10020-10043, 10060-10146	Cal BC8197–8111, 8094–8071, 8066–8037, **8014–7731(0.815)**	
NAV4	NAV4.27	Beta-430522	organic sediment	316	- 103	6720 ± 40	- 27.0	7509-7543, **7559–7668(0.799)**	Cal BC **5719–5610(0.799)**, 5594-5560	0.36
NAV4	NAV4.19	Beta-421844	organic sediment	355	- 142	7880 ± 30	- 27.5	**8590–8778(0.943)**, 883–8860, 8889–8890, 8919–8937, 8960-8972	Cal BC 7023–7011, 6988–6970, 6941–6940, 6911–6884, **6829–6641 (0.943)**	
S 62	S 62.5.1.1	ICEN-770	peat	444	+56	1780 ± 50	- 27.93	**1544–1750(0.951)**, 1759–1792, 1810–1819	Cal AD 131–140, 158–191, **200–406(0.951)**	
ST1	ST1.EII	Beta-373413	organic sediment	1–2	−1/-2	3550 ± 30	- 27.1	3721-3798, **3818–3924(0.658)**, 3949–3962	Cal BC 2013–2000, **1975–1869(0.658)**, 1849-1772	0.26 0.12
ST1	ST1.EXI	Beta-373414	organic sediment	17–20	−17/-20	4060 ± 30	- 27.8	**4422–4621(0.928)**, 4683–689, 4762–4792	Cal BC 2843–2813, 2740–2734, **2672–2473 (0.928)**	
ST1	ST1. EXVII	Beta-373415	organic sediment	31–32	−31/-32	4860 ± 30	- 28.2	5482-5514, 5517–5526, **5575–5608(0.635)**, 5621-5656	Cal BC 3707–3672, **3659–3626(0.635)**, 3577–3568, 3565-3533	
ST2	ST2	Beta-343355	organic sediment	30	−30	4750 ± 30	- 27.1	5330-5378, **5456–5583(0.855)**	Cal BC **3634–3507(0.855)**, 3429-3381	

3.2. Sedimentary analysis

The sedimentary characterization was carried out in the three cores. Sedimentological analyses comprised the textural groups - relative frequency of gravel, sand, silt/clay (mud) - and the grain size. Samples were dried at 40 °C and weighed. Grain size analysis was performed with a combination of dry sieving (>63 μm) and Sedigraph (<63 μm). Samples <63 μm were pre-treated with $(NaPO_3)_6$ at 10% for deflocculating. After washing and drying, a solution was prepared for the analysis in the Sedigraph. The laboratory routines were done according to Tucker (1988). Statistical parameters were determined using *Sedmac* software (Henriques, 2004). The Folk and Ward (1957) method was used for grain size analysis and the textural analysis of sediments was done according to Folk (1954). The sediment genesis was based on Friedman (1967, 1979).

3.3. Radiocarbon dating

A total of thirteen samples were dated. Organic sediments were radiocarbon dated by Beta Analytic and ICA (Table 1). The dating of sediments was done by AMS on organic matter. The calibration of the dates was performed with the program CALIB Rev 8.2 program and IntCal20 data set (Stuiver et al., 2021).

3.4. Palynology

The palynological analysis was performed on the more organic upper part, from the 72 cm–356 cm depth of the NAV-1 core and on two isolated samples (Fig. 2) correspondent to the base and top of a peat that were dated (samples NAV1.23 and NAV1.46, Table 1). Samples were prepared for pollen analysis using standard palynological methods (Moore et al., 1991). TILIA 1.7.14 software (Grimm, 1990–2015) was used for calculation and graphical display of the results. The first column of the diagram shows the sample position and its maximal depth. Percentages of non-aquatic taxa were calculated relative to the terrestrial pollen sum including trees, shrubs, upland herbs and terrestrial vascular cryptogams. Pollen percentages of all aquatic plants (aquatic vascular cryptogams included) were calculated using a total pollen sum. The result of both sums is represented in the final part of the diagram.

Pollen diagrams were zoned using constrained incremental sum of squares (CONISS) cluster analysis. In addition, the results obtained in the two isolated samples are presented in Table 2. It shows the percentages of each identified pollen type and the partial and total sums.

3.5. Ground penetrating radar (GPR)

Several GPR profiles were done, but only S–N profiles 4 and 5 were considered (Fig. 1).

GPR data were collected in common-offset mode every 4 cm using a GSSY SIR3000 GPR system, equipped with a 200 MHz antenna. The system data acquisition was triggered by an odometer wheel, with a time window of 200 ns.

The center frequency of 200 MHz was selected to provide the depth range of the entire sedimentary sequence (up to 10 m) and optimize the vertical resolution to distinguish stratigraphic boundaries and internal reflection patterns. All GPR data were processed with ReflexW software, using standard techniques including dewowing, frequency filtering, manual gain control and topographic correction when needed.

3.6. Historical and archaeological sources

Several historical and archaeological documents were analysed. In

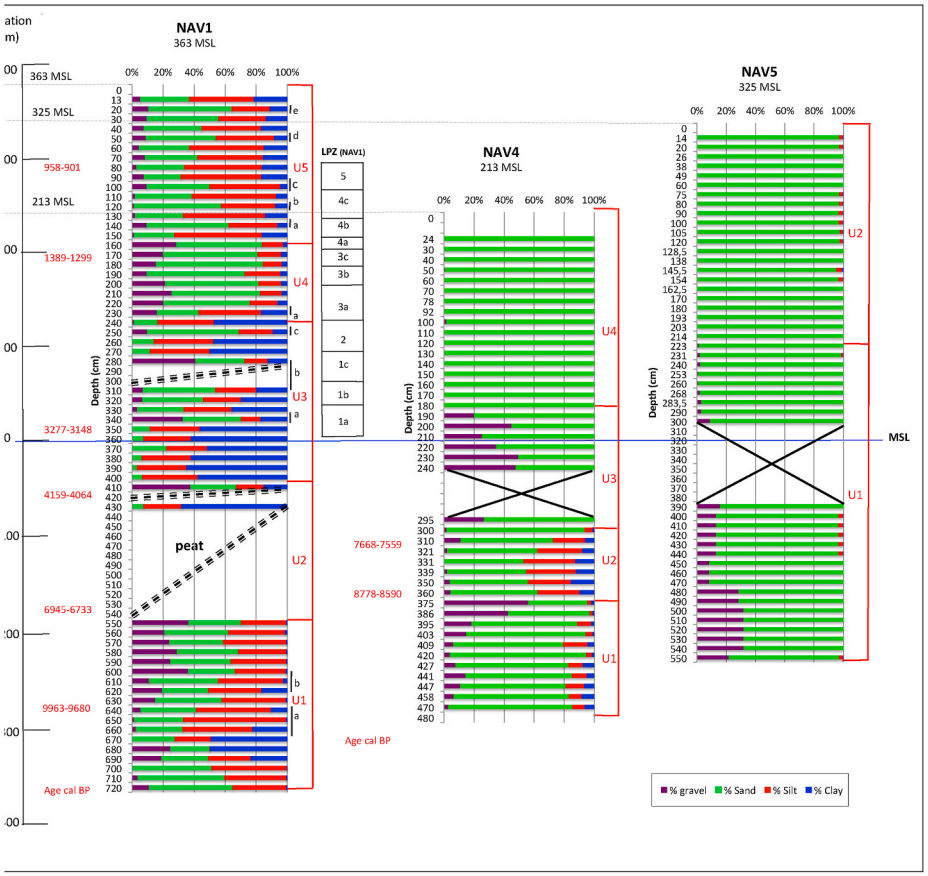

Fig. 2. Sedimentary units, according to the relative proportion of gravel + sand and silt + clay, in cores NAV1, NAV4 and NAV5.

Table 2
Results of the pollen analysis of the samples NAV1.23 and NAV1.46, the percentage of each of the identified pollen types and of the partial sums are shown. (AP/NAP - represents the relationship between arboreal and non-arboreal pollen).

Taxa	NAV1.23	NAV1.46
Pinus (undiff.)	0	1
Quercus robur-type	193	150
Quercus ilex-type	7	12
Corylus	6	4
Betula	2	1
Ulmus	3	0
Castanea	3	2
Alnus	116	181
Fraxinus	3	7
Ilex	3	2
TOTAL arboreal pollen	**336**	**360**
AP/NAP (%)	**87%**	**76%**
Ulex-type	0	1
Erica (undiff.)	4	6
Myrica	0	3
Poaceae	33	10
Compositae liguliflorae	4	0
Compositae tubuliflorae	1	0
Plantago	2	8
Leguminosae	4	2
Caryophyllaceae	0	1
Cruciferae	2	9
Campanula	0	1
Rosaceae	0	1
TOTAL non-arboreal pollen	**50**	**111**
Cyperaceae	18	20
Sanguisorba	0	3
Umbelliferae	14	31
Isoetes	1	3
Ranunculus	2	9
Potamogeton	1	2
Nymphaea	1	2
Total aquatic pollen	**37**	**70**
Spores trilete-type	4	3
Total spores	**4**	**3**
Total terrestrial pollen Sum	**386**	**471**
Total pollen & spores Sum	**427**	**544**

the Northwest peninsular context, the sources are scarce. Some information about geographical descriptions, ethnography or economic development were taken from the texts of Roman or local authors, such as Pomponius Mela, Claudius Ptolemaeus, Gaius Plinius Secundus (Pliny the Elder), Silius Italicus, Pompeius Trogus, Marcial, Orosius, Ausonius, Hidacius, Martin of Dume or monk Egeria (Naveiro López, 1991; Morais, 2005).

The main local historical sources available were produced by monarchs and the Church, including royal charters, archives, inventories (*tombos*) and chancellery records, monastery documents and inquiries. These historical documents have been used by other authors cited in this text. Other archaeological sources used are from co-investigators Morais (2013, 2020) and Oliveira et al. (2013, 2015).

4. Results

4.1. Sedimentary facies characterization

4.1.1. The sedimentological units

Sedimentological units (U) were defined according to the major textural groups.

4.1.1.1. NAV1 (363 cm MSL). Core NAV1, 720 cm long up to the bedrock, presents 5 main units (U1–U5) (Fig. 2) comprising all of the Holocene. In U1, over the weathered schist, there is a hard ferruginous layer at 660 cm depth.

U1, as a whole, has >50% of gravel and sand and extends from 720 cm to 545 cm depth. It is a gravelly muddy sand and a gravelly mud. This unit includes two sub-units of different composition where mud is >50%: U1a from 671 to 645 cm depth and U1b from 622 to 607 cm depth. Unit U1, as a whole, presents one fining (pre-Holocene) and one coarsening up set. U2 is a peat and extends from 545 cm to 405 cm depth. It presents some thin layers of mud and muddy gravel at the top. U3, as a whole, has >50% of mud and extends from 405 cm to 240 cm depth. It is a mud and a sandy mud. It presents three layers with >50% of gravel and sand: U3a at 345 cm, U3b from 312 cm to 275 cm (with an intercalated peaty layer) and U3c at 250 cm depth. U3 corresponds to a sheltered environment where three pulses of higher energy took place (U3a, U3b and U3c). U4 has >50% of gravel and sand and extends from 240 to 160 cm depth. It is a gravelly muddy sand. U4 corresponds to a high energy environment. The 234 cm depth presents a layer with a higher mud content. U5, as a whole, has >50% of mud, extending from 160 cm to the top. It is a sandy mud and a gravelly mud. It presents some thin layers >50% of gravel and sand: U5a at 135 cm, U5b at 120 cm, U5c from 102 cm to 96 cm, U5d at 58 cm and U5e at 16 cm depth.

The thin layers inside main units U, enriched with gravel and sand or silt and clay, respectively correspond to shorter events of more or less energetic dynamics, affecting the dominant hydro-sedimentary conditions of each environment.

4.1.1.2. NAV4 (213 cm MSL). Core NAV4, 480 cm long up to the bedrock, presents four main units: U1, U2, U3 and U4 (Fig. 2). The base of U1 presented quartzite pebbles over the schist.

U1 has >75% sand and gravel and extends from the base to 375 cm depth; it is a gravelly muddy sand and a slightly gravelly muddy sand. U2 has circa 50% of sand and gravel but >25% of mud, and extends from 375 to 305 cm depth; it is a muddy sand. U3 has 100% of sand and gravel, was partially lost during coring, and extends from 300 cm to 180 cm depth; it is a sandy gravel. U4 has 100% sand and extends from 180 cm depth to the surface; it is a sand.

4.1.1.3. NAV5 (325 cm MSL). Core NAV5, 550 cm long up to the bedrock, presents two main units: U1 and U2 (Fig. 2).

U1 is mostly 100% sand and gravel with some thin layers with <5% of mud and extends from the base to 214 cm depth; it is a gravelly sand. U2 is mostly 100% sand with some thin layers with <5% of mud; it is a sand.

4.1.2. Sediment characterization by statistical methods

Sediments were characterized by the mean, sorting, skewness and kurtosis (Fig. 3). With those parameters the dynamics of the environment and the sediment genesis were inferred.

4.1.2.1. NAV1. Sediments are intercalated with mainly fine to very fine sands and silts. All sediments present high values of standard deviation, meaning extremely (some layers of unit U1) to very poorly and poorly sorted sediments.

The mean along the core is very irregular varying between 8.16 and 0.83 (the coarsest thin layer); standard deviation presents values between 4.53 and 1.64; asymmetry is very irregular, with positive and negative alternation, meaning a curve tail on fine and coarse sediments respectively. According to Friedman (1967, 1979), sediments of NAV1 have a fluvial origin (Fig. 4).

4.1.2.2. NAV4. In U1, the standard deviation from 375 cm depth to the base is higher than 1.0, the sediments being poorly to very poorly sorted, with positive asymmetry. There is fine to median and coarse sand alternation (Fig. 3). In U2, the standard deviation from 375 cm to 305 cm is moderately to moderately well sorted. Sediments are mainly very fine to fine sands poorly sorted, with positive asymmetry. The contact

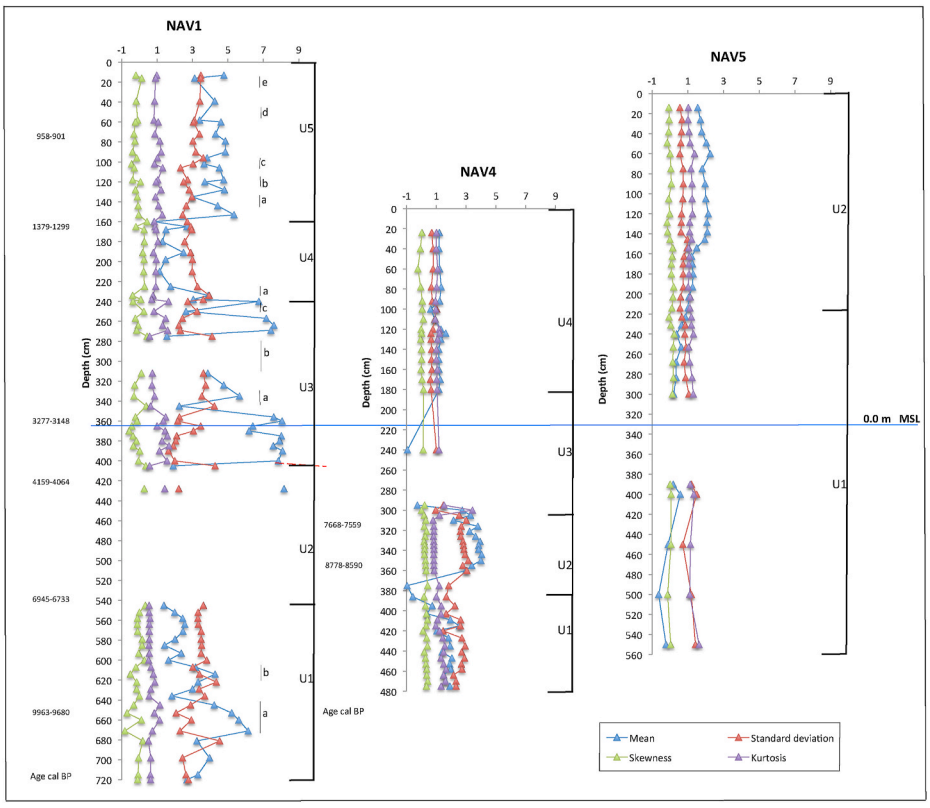

Fig. 3. Folk and Ward statistical parameters of cores NAV1, NAV4 and NAV5.

between U1 and U2 is a very coarse sand, very poorly sorted. According to Friedman (1967, 1979), U1 and U2 are interpreted as fluvial (Fig. 4). U3 (most sediments were lost during coring) is a very coarse sand, very poorly sorted, in sharp contact with U2. U4 is an alternation of median and coarse sand, moderately to well moderately sorted.

4.1.2.3. NAV5. U1 is very coarse sand passing to coarse sand poorly and moderately sorted. U2 has an alternation of median and fine sand moderately or moderately well sorted.

4.1.3. Environmental evolution from sedimentological data

4.1.3.1. NAV1. Considering the units identified through the main composition of their sediments, four clusters can be recognized (Fig. 5 A), pointing to a succession of different sedimentary and energetic environments:

(i) a gravelly muddy sand and gravelly mud cluster represented by U1, concerning a high energy environment, with two main levels (U1a and U1b) of finer sediments concerning temporary accentuated dynamics decrease; (ii) a mud and sandy mud cluster represented by U3, with a decrease in energy relative to U1, concerning a quiet environment with three higher energy pulses represented by coarser sediments (U3a, U3b and U3c, Fig. 2); (iii) a gravelly muddy sand cluster represented by U4, concerning a gravel input and higher dynamics; (iv) and a sandy/gravelly mud represented by U5, concerning a decrease in dynamics relative to U4.

The clusters represent four main environments corresponding to a decrease in energy from U1 to U3 passing to higher energy in U4, which decreases again in U5, partially overlapping U1 conditions (Fig. 5 A). U2, an organic peat, corresponding to a quiet phase between U1 and U3, was not considered in this analysis. The sedimentation rates (mm/yr) increase over time, being 0.35 (U1), 0.44 (U2), 0.71 (U3 lower), 1.00 (U3 upper and U4) and 2.34 (U4 upper and U5) (Table 1).

4.1.3.2. NAV4. Four clusters can be identified – a gravelly and a slightly gravelly muddy sand (U1), a muddy sand (U2), a sandy gravel (U3) and a sand (U4), meaning a decrease in energy from U1 to U2, followed by an increase from U2 to U3 and another decrease to U4. U3 and U4 represent higher energy than U1 and U2 (Fig. 5 B). The sedimentation rate is 0.36 mm/yr between 8778-8590 cal BP and 7668-7559 cal BP (U1 and U2), the same rate as U1 of NAV1 (Table 1).

4.1.3.3. NAV5. Two clusters can be identified, a gravelly sand (U1) and a sand (U2), both representing high energy events, though with decreasing intensity from U1 to U2 (Fig. 5 B).

4.2. Geochronology

Four sediment samples from NAV1 and two from NAV4 were radiocarbon dated in order to establish a chronological framework for the palaeoestuary (Table 1).

In NAV1, the most basal dating at −282cm MSL is 9963–9680 cal BP. At −177cm MSL is 6945–6733 cal BP, at −57cm MSL is 4159–4064 cal BP cal BP, at +7 cm MSL is 3277–3148 cal BP, at +195 cm MSL is 1379–1299 cal BP and at +291 cm MSL is 958–901 cal BP.

In NAV4, two dates were obtained, one at −142cm MSL of 8778–8590 cal BP and another at −103cm MSL of 7668–7559 cal BP.

With data (Table 1) from this work and from Rio de Moinhos (Granja et al., 2016) and S 62 (Granja, 1999), an elevation (MSL) *versus* age graph of the dated organic sediments was constructed for this geographical zone. Two curves, one (A, on the east side) from cores NAV1 and S62 and the other (B, on the west side) from cores NAV4 and ST were considered. Linear regression equations and the respective plots were calculated independently for both curves. Curve A has $r^2 = 0.9956$ on the lower and $r^2 = 0.9732$ on the upper segments of the profile. Curve B has $r^2 = 0.9814$ (Fig. 8).

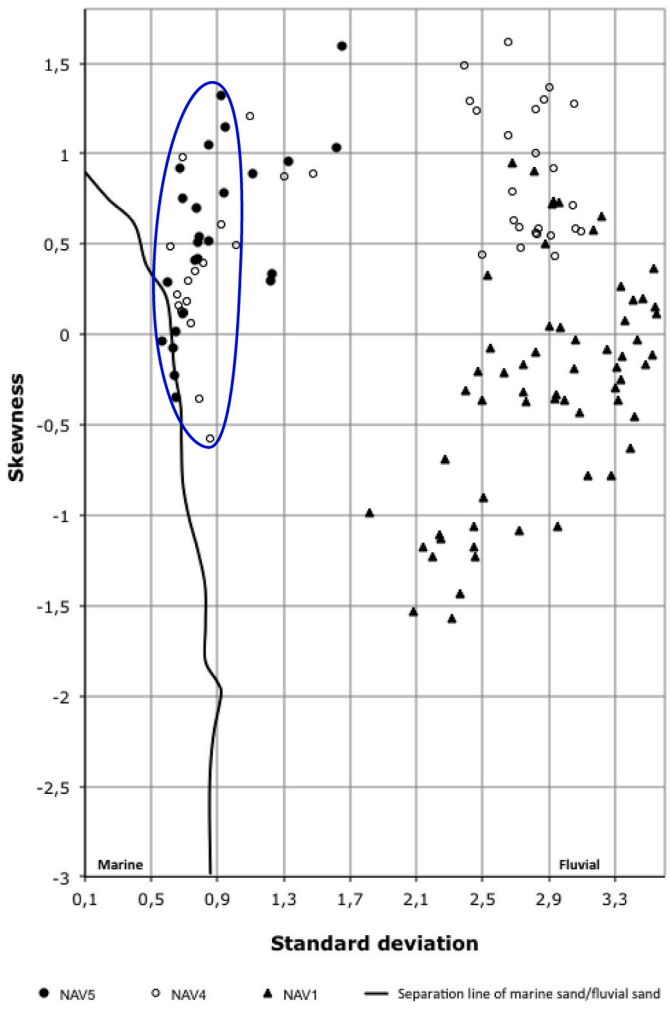

Fig. 4. Sediment genesis of cores NAV1, NAV4 and NAV5 according to the Friedman plot standard deviation/asymmetry.

4.3. Palynology (core NAV1)

The two single samples analysed were dated respectively to 6945-6733 cal BP (NAV1.23) and 4159-4064 cal BP (NAV1.46) (Table 2). These dates place the samples around the moment of the appearance of agriculture in the territory (Ramil-Rego, 1992; Ramil-Rego et al., 2015). In both samples, a moment of arboreal dominance is reflected (Table 2), with an important representation of the humid forests associated with the environment of the wetland (*Alnus*). *Pinus* is only present in the most modern sample, represented by a single pollen grain (Table 2).

The pollen diagram (Figs. 6 and 7) represents the substitution of *Quercus robur* type by *Pinus pinaster* type. Concerning the local vegetation, from the wetland, there are different phases of development of a net continental wetland dominated by freshwater. The dates indicate this process occurred between the Bronze Age (circa 4000-2300 cal BP) and the end of the High Middle Age (11th century). The sequence comprises 5 pollen zones (Figs. 2, 6 and 7).

4.3.1. LPZ-1 (356 cm–275 cm)

The base of the zone was dated in 3277–3148 cal BP (1328-1199 cal BC). This zone represents a landscape in a deforestation phase (Fig. 8), reflecting the successive intensification of anthropization, that has characterized the last third of the Holocene in NW Iberia (Mateus, 1992; Muñoz Sobrino et al., 2005; Ramil-Rego et al., 2009; etc.). Cerealia is present from the base of the sequence as numerous taxa associated with agricultural activity (*Asphodelus, Plantago*, Cruciferae or Leguminosae).

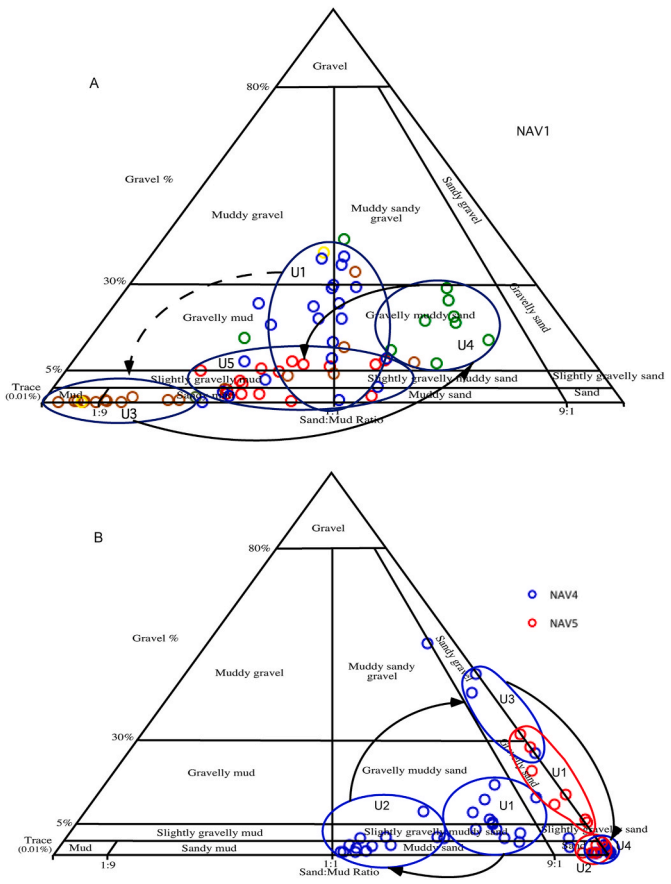

Fig. 5. Spatial and temporal distribution of sedimentary unit clusters of core NAV1 (5 A) and of cores NAV4 and NAV5 (5 B). Classification of major textural groups according to Folk (1954).

The regional vegetation would have been represented by open landscapes of heathlands and small zones of oak forest (Fig. 6). The sub-zones LPZ-1a and LPZ-1c represent forest development and LPZ-1b represents forest detriment. The parallel dynamics of *Alnus* in this zone indicate that the oak groves were related to the wetland surroundings, as in Rio de Moinhos (Granja et al., 2016).

The local vegetation implies the existence of a freshwater wetland, with high species diversity (*Isoetes, Sphagnum, Ranunculus, Cyperaceae, Alisma*, *Nymphaea*, *Myriophyllum* or *Potamogetom*). The LPZ-1b zone shows a small reduction in these elements and an expansion of *Myrica,* and the LPZ 1c shows a small increase of *Nymphaea* and *Myriophyllum* (Fig. 9).

4.3.2. LPZ-2 (275 cm–240 cm)

Zone 2 corresponds to a strong detriment of oak (Fig. 8). Other arboreal taxa such as *Betula* and *Alnus,* related to wetland environments, were also reduced. The zone corresponds to the beginning of the continued curve of *Cerealia*. The vegetation of the wetland is practically the same as that of the end of LPZ-1, except for a small increase in *Cyperaceae* (Fig. 9).

4.3.3. LPZ-3 (240 cm–168 cm)

Zone 3 represents a new detriment of *Quercus robur*-type, a succession of two increases in *Pinus pinaster*-type and finally a strong reduction in this taxon. Sub-zones 3a and 3 b show sudden increases in Pinus. Subzone 3c is marked by a sharp fall in *Pinus*. Zone 3 (1379-1299 cal BP; 571–651 cal AD) in turn represents an increase in Cerealia and some taxa linked to synanthropic environments such as *Asphodelus*, *Plantago* or *Tubuliflorae*. The vegetation of the wetland shows an initial rebound

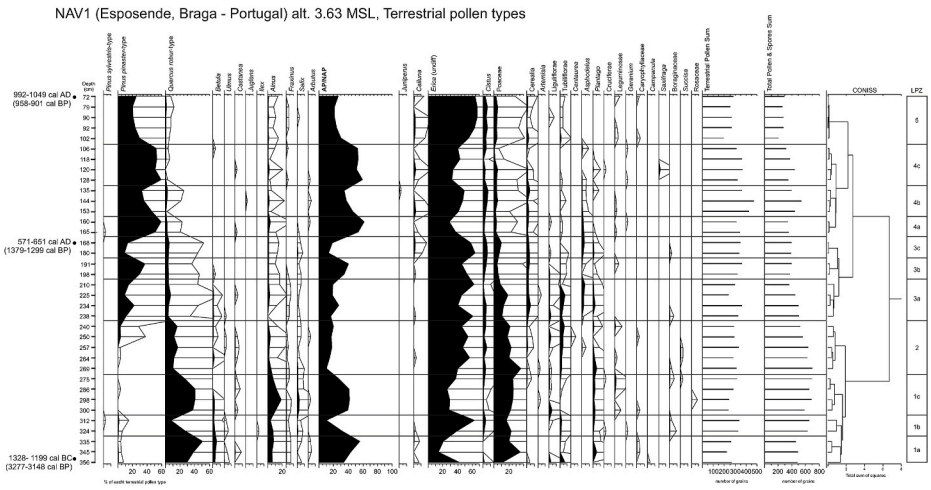

Fig. 6. Chronology, zones and pollen percentages diagram of the NAV1 section analysed. Terrestrial pollen types. (AP/NAP: represents the relationship between arboreal and non-arboreal pollen; LPZ local pollen zones).

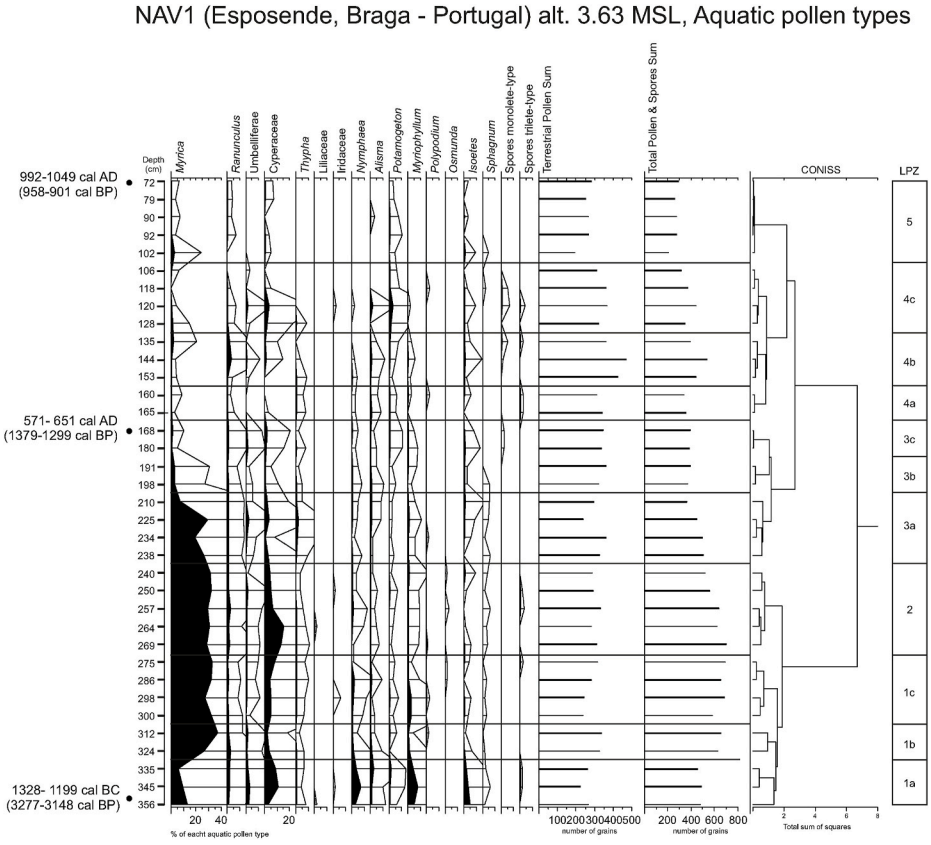

Fig. 7. Chronology, zones and pollen percentages diagram of the NAV1 section analysed. Aquatic pollen types.

of *Myrica*, followed by a strong detriment of this taxa, while the rest of the aquatic taxa maintain their dynamics (Fig. 9).

4.3.4. LPZ-4 (168 cm–106 cm)

This zone reflects the maximum expansion of *Pinus* (Fig, 8), with two maximums (LPZ-4a, 4c) separated by a short backward phase (LPZ-4b). The dynamics of the aquatic taxa do not reflect notable changes with respect to the previous zone (Fig. 9).

4.3.5. LPZ-5 (106 cm–72 cm)

This zone (958-901 cal BP; 992–1049 cal AD) shows a sharp decline in the *Pinus* curve. The vegetation of the wetland reflects a decrease in the diversity of aquatic taxa and the disappearance of *Nymphaea*, *Myriophyllum* or *Alisma*.

4.4. Georadar (GPR)

A strong reflector can be observed circa 200 cm depth, probably corresponding to the water table (Fig. 9). Below the surface, reflection standards of sandy formations are observable. On profile 4 (Fig. 9 A), this structure is near 200 cm depth gradually increasing to 600–700 cm northwards in front of the Bonança chapel. On profile 5 (Fig. 9 B), inside

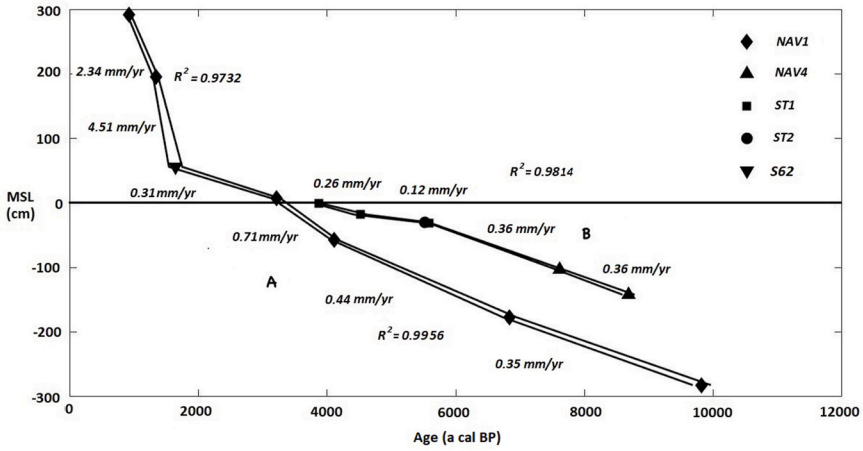

Fig. 8. Depth *versus* Age (a cal BP) graph of the dated sediments of the Cávado (NAV1, NAV3, NAV4 of this work; and S62 from Granja, 1999) and Rio de Moinhos, Esposende (ST1 and ST2, Granja et al., 2016) and sedimentation rates (mm/yr).
The linear regression equations and the respective plots were computed independently, for the lower and upper segments of the profiles.

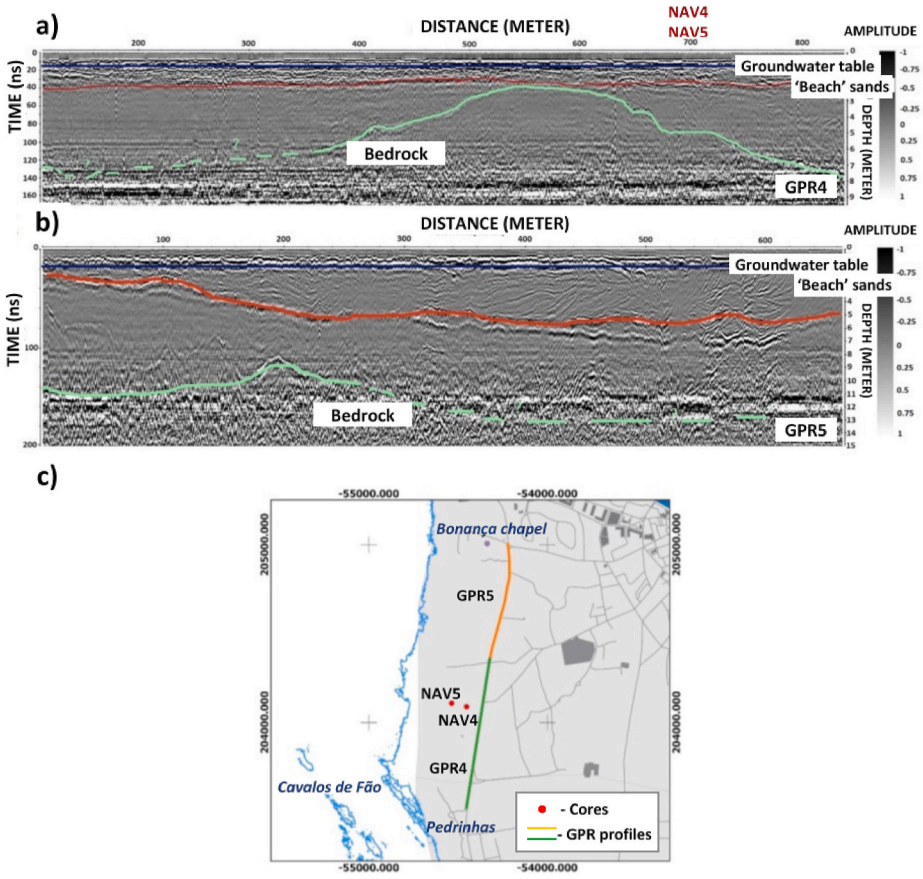

Fig. 9. South-North ground penetrating radar (GPR) profiles at Bonança (Esposende). A: GPR profile 4 and location of cores NAV4 and NAV5; B: GPR profile 5; C: location sketch.
The green line indicates the bedrock limit; the red line indicates the lower limit of probable marine sands; and the blue line indicates the groundwater table. Coordinates: Datum ETRS89 Portugal TM06. . (For interpretation of the references to colour in this figure legend, the reader is referred to the Web version of this article.)

this structure, reflection geometry compatible with cross stratification is observable.

Under this unit, several reflections of variable width were detected. Profile 4 presents reflections between 400 and 800 m that may be due to coarse sandy units or sands with gravels, which seem to continue along profile 5.

The bedrock was identified by the presence of a strong reflector of irregular geometry, at different depths. On profile 4 (Fig. 9 A), at Pedrinhas, the bedrock is at 800 cm depth, and gradually rises northwards to 300 cm depth. At 550 m, the bedrock plunges again. At the North boundary of profile 4, the bedrock is at 700 cm depth and plunges North through profile 5 until its reflection is no longer perceptible (it is likely deeper than 1000 cm in depth).

On both GPR profiles (Fig. 9 A and B), the bedrock surface is irregular, presenting two main E-W broadly oriented incisions between Pedrinhas and Bonança (Fig. 9 C), that suggest former river channels, as indicated in historical documents. Cores NAV4 and NAV5 were done on the border of one of these channels (Fig. 9 A).

4.5. Historical and archaeological background

The position of the former inlet of the Cávado river, somewhere southwards of the present one, is still an on-going study. Several historical texts point to the inlet at Fam (Fão, Fig. 1 A and C), an important trade site dedicated to salt exploitation and fishery.

Around 3000 cal BP, the Castro culture arose with communities choosing high points to settle. The most significant examples of the commercial routes in the pre-Roman period are represented by the coastal fortified settlements, situated in important places and in the estuaries of important rivers, such as the settlements of Coaña, Sta. Trega, Sta. Luzia, Terroso, Bagunte and Vila Nova de Gaia (Naveiro López, 1991). The importance of another smaller settlement situated in a perched position by the mouth of the Cávado River should also be emphasized - the settlement of S. Lourenço. It is situated at Esposende, a position relatively close to *Bracara Augusta* (present Braga, Fig. 1), which can be inserted in the context of the maritime-river trade of the Atlantic as a result of the archaeological remains thus far found – among which there is an attic red-figure ceramic fragment from the 4th century BC (Almeida and Cunha, 1997). The S. Lourenço castro, on the top of the dead cliff at Esposende (Fig. 1 A), had its apogee between the 1st century BC and the 1st century AD. During the 5th century AD, it was abandoned. Salt was an important economic commodity for Castro populations. It was exploited in the Cávado estuary, especially in Fam, but also in Gandra and North of Esposende (Almeida, 2005).

This strong connection to the sea is not only cited by the historical sources focusing on salt exploitation and trade. Several Roman shipwreck remains have been documented over the last decades, like numerous amphorae from *Baetica* dated from the Augustan period (Morais, 2013). The chromatographic analysis performed on fragments of some amphorae revealed extensive pine resin remains together with traces of wine and olive oil, suggesting the waterproofing of these ceramic containers and their use in the transport of *defructum* (Morais, 2013; Oliveira et al., 2015). Very probably, this cargo was destined for the S. Lourenço castro, where many amphorae fragments were found (Almeida, 2006), demonstrating the role of this settlement in the Atlantic marine-fluvial trade (Morais, 2005).

Several researchers have dedicated themselves to the compilation and interpretation of the historical manuscripts. In the discussion of this work, data from these authors has been used in an attempt to frame the palaeoestuary evolution during the Late Holocene within the history of Esposende.

5. Discussion

The sedimentary facies, the palynological sequence, the historical and archaeological information, the geophysical data and some radiocarbon dates have been used to build the palaeoenvironmental evolution of the Cávado estuary from the Early Holocene up to historical times (Fig. 10). Interpolation with previous data and comparison with data from other Iberian estuaries has been done to improve the local evolution model (in the absence of other ecological and chemical data).

5.1. Early Holocene

The base of NAV1 has very poorly sorted fine sediments - sandy mud -

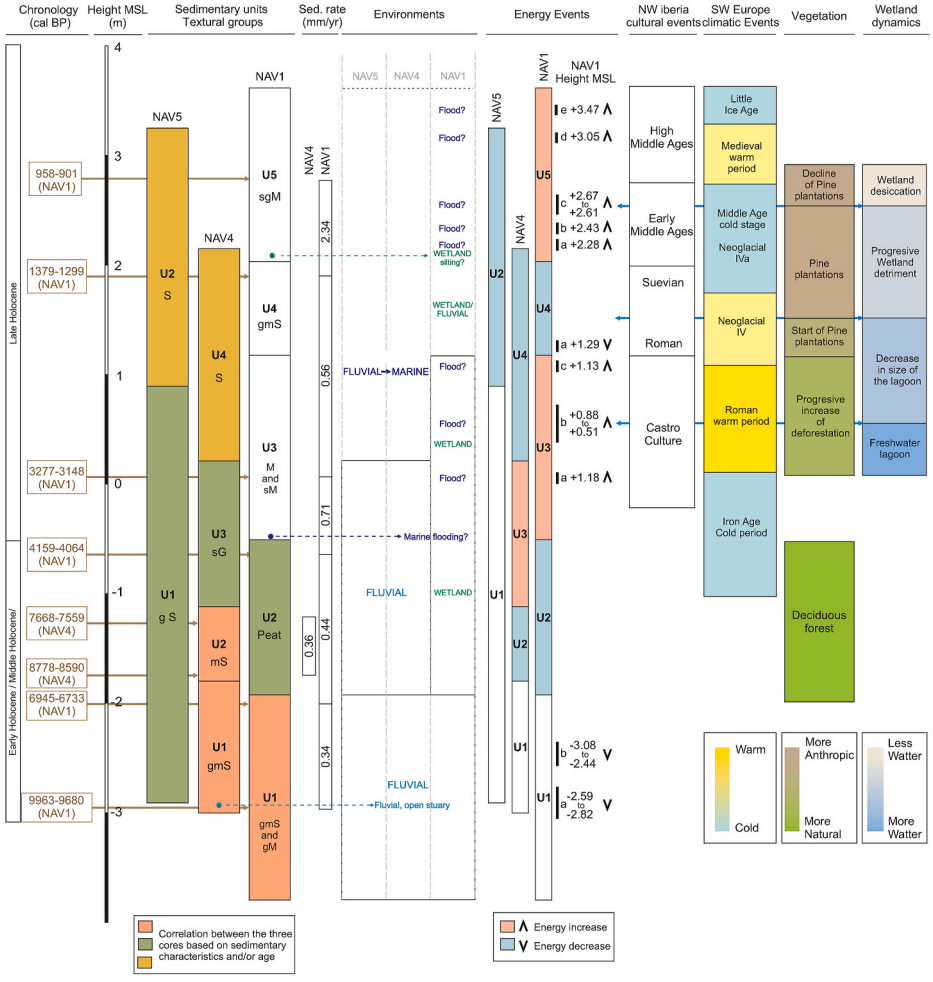

Fig. 10. Synthesis chart of Holocene palaeoenvironmental evolution of the Cávado estuary. From left to right: the chronology; the MSL scale; the sedimentary units and the textural groups (sgM: sandy gravelly mud; gmS: gravelly muddy sand; M: mud; sM: sandy mud; gM: gravelly mud; mS: muddy sand; S: sand; gS: gravelly sand; sG: sandy gravel); the sedimentation rates; the environmental evolution; the energy events; the cultural events of the NW Iberia; the climatic events of SW Europe for the end of the Holocene; the vegetation of the area; and the dynamics of the wetland of the upper part of NAV1 (U3, U4 and U5).

in a fining upward set, representing a decrease in fluid velocity within a fluvial channel. The ferruginous hard level at −297 cm MSL, older than 9963 cal BP, is interpreted as an indicator of sub-aerial exposure of former sediments under a subsequent cold and probably dry phase (Younger Dryas; see Rodrigues et al., 1991).

The Early Holocene sediments aged 9963-9680 cal BP are located at −282 cm MSL (Fig. 2). They constitute a succession of gravelly mud and gravelly muddy sand corresponding to a general increase in energy (Fig. 5). This is probably related to river infill with reworked former fluvial/marine sediments and mud coming from soil erosion, under warm and wet conditions (insolation maxima and precession minimum, Gomes et al., 2020) and sea level rise. This succession presents two levels of finer sediments concerning events of quitter dynamics, one before 9963 cal BP and the other after 9680 cal BP (Fig. 2).

The sediments of NAV4 and NAV5 are much coarser than those of NAV1 meaning that the dynamics were much more energetic at Bonança, closer to the sea and exposed on the border of a river channel (Fig. 9 A). At the base of NAV4, pebbles are present (pebbles are frequent over the shore platform; Granja et al., 2016).

NAV4 (Fig. 2) presents pebbles and a gravelly muddy sand (U1) over the bedrock, overlapped through sharp contact by a muddy sand (U2) aged from more than 8778–8590 up to 7668-7559 cal BP. It could be interpreted as a succession of different hydrodynamic flow conditions or a lateral migration of the channel with subsequent sedimentary facies change. The transition from Early to Middle Holocene occurs within U2 of NAV4.

The basal sediments of NAV5 (Fig. 5) are a gravelly sand, corresponding to a still more energetic and exposed environment than that of NAV4. U1, with poorly calibrated coarse sands, fining up, is interpreted as an energetic fluvial environment (Figs. 3 and 4).

The period 9800-7400 cal BP is characterized by optimum temperature and precipitation conditions in NW Iberia (Gomes et al., 2020), which would have favoured the increase of fluvial flow. During this period, the climatic sequences register two abrupt cooling phases, dated around 9300 cal BP and 8200 cal BP (Rasmussen et al., 2014). The data available for the early Holocene in NW Portugal show that these abrupt events would have affected both the interior mountains (Lagoa de Marinho, Ramil-Rego et al., 1998) as well as those closest to the coast (Serra da Arga, Gómez-Orellana et al., 2010). In all three cores, the gravel content increases (Fig. 2).

The sedimentation rate in this period was 0.35 mm/yr (Table 1, Fig. 8). This is much lower than that of other Portuguese, albeit deeper, estuaries (e.g. Guadiana with 7.6 mm/yr, Boski et al., 2008).

5.2. Middle Holocene

During the Middle Holocene, between 8000 and 5300 cal BP, the Holocene Climatic Optimum occurred, a phase during summer generally warmer than today in the Northern Hemisphere. Between 6945 and 4064 cal BP, a peat (U2 of NAV1) more than 150 cm thick accumulated in NAV1. On the top of the peat, some thin layers of poorly sorted sands are present (Fig. 2). This period favoured by the deceleration of sea level rise) is characterized by peat deposition at mid latitudes (Muñoz Sobrino et al., 2005) and the filling of plains (Baeteman, 1999).

The pollen data obtained from the base and top of this peaty layer (Fig. 2, Table 2) show the dominance of the arboreal formations, represented by oak groves and forests dominated by *Alnus*, the latter related to the surrounding forests of the wetland. This period is related to the end of the Holocene Climatic Optimum. The oldest pollen sample has a slightly higher percentage of trees and a greater representation of oak groves, which represent regional forests. This difference represents a greater anthropization of the territory, which does not affect the forests related to the wetland. The remaining values determine that, despite the increase in the anthropization of the territory, both local and regional forests would maintain an important representation in the landscape.

During the Middle Holocene, the sedimentation rate was 0.44 mm/yr eastwards (similar to that of e. g. Estremadura, 0.3–0.4 mm/yr, Ramos-Pereira et al., 2019) and circa 0.36 mm/yr and 0.12 mm/yr westwards (Fig. 8).

5.3. Late Holocene

5.3.1. Pre-Roman (Castro culture)

NAV1 was taken very close to another core (Granja, 1999) that will be used for complementary interpretation (referred to here as S62, Fig. 1, Table 1). If the two cores correspond, the disturbed top of U2, with poorly sorted sands evidencing high energetic events, probably concerns the sudden flooding of the upper saltmarsh referred to in Granja (1999). This would mean that, after a progressive freshwater influence in the environment, a sudden increase of marine influence (-24.6 $\delta^{13}C$, NAV1.58, Table 1) took place somewhere between 4159-4064 cal BP and 3277-3148 cal BP (there is a sharp contact between U2 and U3, Figs. 2 and 3). After this episode, the freshwater conditions would have prevailed again until a terrestrial environment. Very probably U3, U4 and U5 correspond to the two upper sections of S62 (transition from a brackish stagnant lagoon to an upper marsh, Granja, 1999), which is in accordance with the pollinic data of the present work.

What could have motivated the inversion of the general trend of freshwater conditions somewhere before 3277-3148 cal BP? A high-energy event such as a big storm? It doesn't seem probable that the event occurred during the period 5000-4000 cal BP (Middle Holocene), when rates of sea level rise were strongly attenuated (different ages have been proposed; see e. g. Boski et al., 2008; Leorri et al., 2012; Sousa et al., 2018). However, if the event happened during the period of polar cooling of 4200–3000 cal BP (Mayevsky et al., 2004) favouring storminess, it would be acceptable. Furthermore, according to González-Villanueva et al. (2015) storm events along NW Europe seem to be in phase with the Holocene cooling events documented by Bond et al. (1997).

Around 3000 cal BP, Neoglacial conditions would prevail (Wang et al., 2012), with 3300 and 2800 cal BP corresponding to general cooling periods in the North Atlantic (Solomina et al., 2015), 3500–2500 cal BP to "cool poles, dry tropics'' pattern postulating that solar variability could be a plausible forcing (Mayewski et al., 2004).

However, at Rio de Moinhos, a lagoon sediment dated 3924-3818 cal BP is clearly truncated at the top (Granja et al., 2016). This truncation could be related to marine flooding and overwashing as described by González-Villanueva et al. (2015) for other coastal wetlands of NW Iberia.

The marine flooding, associated with the prevalence of storminess, that may have occurred at the top of U2 of NAV1 could easily fit in this period of time. Ramos-Pereira et al., (2019) refer to a "wet episode" at 4900-3900 cal BP (in Estremadura) after the sea had reached its present position, but do not point to any marine influence. However, Costa et al. (2019) refer to an increase of marine influence at around 3500 cal BP on the SW Portuguese coast at the Albufeira, Melides and Santo André lagoons. Furthermore, Lario et al. (Costa et al., 2019) refer to a tsunami-related event at that time in the Gulf of Cadiz. With the available data, it is impossible to say what kind of event took place in the Cávado palaeoestuary and its surrounds. At the Minho and Douro estuaries (Fig. 1) such an event has not been described until now.

From 3000 cal BP until the 5th century AD, the Cávado river had a strong connection to the sea. Archaeological sources point to the apogee of Castro St. Lourenço due to salt exploitation in the Cávado estuary (Almeida, 2005). This fact is in accordance with the emergence and development of the Castro culture (Naveiro López, 1991) during the Bronze and Iron Ages.

From 3277-3148 cal BP (1328-1199 cal BC) to 1379-1299 cal BP (571–651 cal AD), the sedimentation rate was 0.31 mm/yr (Fig. 8), very similar to that of other small Portuguese estuaries (e. g. Ramos-Pereira et al., 2019).

In relation to vegetation and landscape, the base of the pollen diagram (LPZ-1, inside U3, mud and sandy mud sediments with a coarse layer corresponding to a higher energy event, Figs. 2 and 6) corresponds to a period of climatic improvement (Roman Warm Period: 2900-1900 cal BP). In NW Iberia, it corresponds to the Bronze Age (circa 4000-2300 cal BP) and Iron Age (2300 cal BP to the 1st century BC). It is a moment of important cultural change with the building of a new model of society, based on sedentary settlement, and organized around productive settlement (Ramil-Rego et al., 2009, 2015).

Favoured by this climatic improvement, there is a progressive increase in the number of settlements related to the expansion of agricultural and cattle practices. This rise implies an increase of human intervention over the landscape, especially on littoral and inner low areas (Ramil-Rego et al., 2009). The footprint of the land use intensification of the territory results in a great deforestation of the surroundings, which produces a landscape where woodland occupies only areas with bad conditions for agricultural practice.

At that time, the local vegetation represented in the pollen diagram (Fig. 9) implies the existence of a freshwater wetland, with high species diversity, representing several ecological environments. Some taxa (*Isoetes, Sphagnum, Ranunculus, Cyperaceae, Alisma*) show the existence of supra-littoral environments with hydrophilic or peaty conditions while others (*Nymphaea*, *Myriophyllum* or *Potamogeton*) are characteristic of freshwater lagoon environments. The maximum representation of these taxa concerns the pollen zone LPZ-1a (Fig. 9). The zone LPZ-1b shows a small reduction of these elements and an expansion of *Myrica,* a typical element of peaty environments. This dynamic reflects the expansion of arboreal and big shrub formations in the wetland, at the same time that the surface of free water reduces. In the LPZ-1c zone the stabilization of this situation occurs, with a small increase in *Nymphaea* and *Myriophyllum*, indicators of pool permanence (Fig. 7).

5.3.2. Roman times

The Roman invasion of the NW Iberia takes place in 2087 cal BP (137–25 BC), during the cooling event that ends the so-called Roman Warm Period (Ramil-Rego et al., 2009; Ramil-Rego and Gómez-Orellana, 2016). In NW Iberia, Romanization is related to a highly anthropized landscape with very few areas of woodland and other pristine territorial environments (Ramil-Rego et al., 2009, 2015; Ramil Rego and Gómez-Orellana, 2016). In other sequences of this period in central and northern Portugal, there is a similar situation (Mateus, 1992; Ramil-Rego et al., 1996, 2016; Gómez-Orellana et al., 2001; 2010; Granja et al., 2016).

NAV4 and NAV5, mainly coarser than NAV1, are located (Figs. 1 and 9) at the border of a channel. The base of U3 of NAV4 and the top of U1 of NAV5, very coarse sands moderately sorted (Fig. 3), may point to marine influence (Fig. 4) in the channel during Roman times.

It is probable that some kind of clastic barrier already existed westwards. The age of the onset of barriers is different according to authors and regions (e.g. 8000-5300 BP at barrier-lagoon systems of NW Iberia, 8500 BP at Formosa lagoon). At the Douro river, between 6530 and 1500 cal BP, a gravel barrier was set in and the main fluvial channel migrated northwards enlarging the estuarine zone (Naughton et al., 2007). At the Minho river, the sand bar that evolved into a dune was set in 3000 cal BP (Leorri et al., 2012).

Regarding the dynamics of the vegetation, the pollen zone LPZ-2 (topmost of U3 from NAV1 with a high energetic event, Fig. 2) could be related to the Roman invasion of NW Iberia. The pollen diagram shows a great decrease of forests, both regional forests and those linked to wetlands, and an increase of Cerealia and some taxa that would be linked to a synanthropic environment (*Asphodelus, Plantago* or *Tubuliflorae*). Both of these represent an increase in deforestation and agricultural practices. This anthropic deforestation favours the development of heathlands, likely including wet heathlands around the wetland.

During Roman times, ca 2000 BP, there is reference to increasing continental erosion (Hoffman, 1989), responsible for the progradation of the coastline in the South of the country (Dias et al., 2000). However, between the 1st century BC and 1st century AD, salt exploitation was at its apogee and the majority of larger gauge Roman vessels cast anchor and watered safe from any hazards in the Cávado estuary, especially in Fam (Morais, 2005). Therefore, it is improbable that continental erosion was very significant in this zone at that time, or if it was, its consequences did not reach the river mouth.

The presence and increase of *Pinus* in the pollen zone LPZ-3 (inside U4, gravelly muddy sand Fig. 2) is probably related to anthropic action. The sudden appearance and rapid increase of this element occurred without other regional changes in taxa. This has led to the inference that the presence and increase of *Pinus* in LPZ-3 (Fig. 6) is associated with human action and the active development of forest plantations for wood or resin purposes.

In the pollen sequences available in NW Iberia for the period between 5200 cal BP and the end of the Middle Ages (1440 AD), the presence of *Pinus* pollen is in most cases testimonial, with the exception of the mountain areas, where it still has a significant presence, although very limited when compared to the territories of the Iberian Plateau or the coastal and sub-coastal territories of the Mediterranean, where pine forests maintained an important representation in the landscape at different stages of the Holocene (Mateus, 1992; Ramil-Rego et al., 1996, 2015; Gómez-Orellana et al., 2001; 2010; Muñoz Sobrino et al., 2005; Granja et al., 2016). If we focus on the coastal and sub-coastal areas of Northern Portugal and Galicia, *Pinus* is a minor element in the vegetation throughout the entire Holocene (Ramil-Rego et al., 1996; Gómez-Orellana et al., 2001; 2010, 2021; Granja et al., 2016). Only in some sequences recovered on the seabed is a greater representation of *Pinus* observed, which responds to an over-representation, linked to the greater rate of transportation that *Pinus* pollen presents in the medium or long distance, compared to that of deciduous species. In the immediate surroundings of the new sequence, the scarce presence of *Pinus* pollen is evidenced in the Holocene sequence of Río de Moinhos (Granja et al., 2016), or in the diagram itself obtained in NAV-1, which at the base of LPZ-3 (mud and sandy mud sediments) represents the Holocene phase of anthropogenic deforestation with the presence of deciduous stands and near absence of *Pinus* (Fig. 8). The scarcity of *Pinus* is also observed in the two single samples analysed in NAV-1 and dated to the middle Holocene (Table 2).

Therefore, the expansion of *Pinus* recorded in the pollen diagram (Fig. 6) does not correspond with the regional dynamics of the territory. It would therefore be a local episode not linked to climatic dynamics that could only be connected with human activity through *Pinus* plantations around the mouth of the Cávado river.

Morais (2013) highlights the important marine-fluvial trade between Baetica and the region of Esposende, during Augustus' time, when the Cávado river was an important Roman anchor point. The coeval morphology points to the existence of a kind of *gulf* enclosed by Cavalos de Fão, the so-called *Cala* (Morais, 2005), and bordered by the promontories of Cepães to the North and Pena-Pedrinhas to the South (Ordovician quartzitic outcrops, Fig. 1). These facts corroborate the importance of the Cávado estuary and coastal surroundings as an anchoring site in Roman times, benefiting from a morphological context with sheltered areas (as happened at Rio de Moinhos and Apúlia (Granja et al., 2010, 2013, 2016). The Fão inlet would be a boat entrance, perhaps not excluding others such as at Rio de Moinhos, where the remains of a probable Roman quay were found (Morais, 2020).

In this sense, the expansion of *Pinus* (LPZ 3a and 3 b) corresponds to plantations of this species that would begin in the final period of the Roman occupation and during the Suevian Kingdom of Gallaecia. These forest plantations would be related to the supply of wood and resin to the shipyards in charge of repairing or building ships for marine or river traffic to the city of Bracara. The hypothesis of the presence of tree plantations to supply shipyards in Roman times was also raised in some areas of the Italian peninsula (Allevato et al., 2009).

With the decline of the Roman empire, *Bracara Augusta* became the

capital of the new Suevian kingdom of *Gallaecia* and economic interests moved. However, even after the abandonment of the *castro*, during the High Middle Age, salt exploitation continued in the Cávado, henceforth controlled by the monasteries (Almeida, 2005).

The pollen diagram (Fig. 6) also shows a marked increase of Cerealia and of some synanthropic taxa at the beginning of the LPZ 3, which corresponds to a strong increase in agricultural activity in the surroundings of the city of Bracara Augusta, in relation to its rise as the capital of the Roman Conventus Bracarensis and of the Suevian kingdom of Gallaecia.

During the Roman and Suevian times, the wetland would present a lower level of flooding and an increase in the vegetal formations of the shoreline of the lagoon.

5.3.3. Medieval (up to the 14th century)

The pollen diagram shows (Subzone 3c) a sharp fall in *Pinus* (Fig. 8), which from the date obtained at that point (571–651 cal AD) could be related to the capture of the city of Braga by Theodoric II in 585 AD and the end of the Suevian Kingdom of Gallaecia and, therefore, of the late medieval splendour of the city of Braga.

From 158 to 972 AD (concerns part of U4 and U5 of NAV1; LPZ-3 and LPZ-4) there was a warm period with an increasing trend in temperature and free ice cover, though some authors point to a short episode ca. 550–600 AD of a windier and dry cooling climate in central Europe (Zalat et al., 2018). Perhaps the abandonment of Castro S. Lourenço during the 5th century AD was a consequence of a similar but earlier episode.

The vegetation dynamics in the pollen diagram (zone LPZ-4: transition U4–U5, from a coarser to finer accentuated increase, though with five pulses of higher energy, Figs. 2 and 6) would correspond to an increase in agricultural activity, also linked to the development of the city of Braga and its surroundings.

Subzone 4 b (includes a coarser sediment layer, Fig. 2) shows a decrease of the *Pinus* plantations (Fig. 6), which may reflect a moment of socio-political instability that could be linked to the time of the arrival of the Arabs in the surroundings of Braga.

The period from 900 to 1240 AD had a warm climate and reduced glacier activity (Wanner et al., 2008). At that time, which corresponds with the top of the pollen sequence (LPZ-5 pollen zone, inside U5, finer sediment increase Figs. 2 and 6), the diagram shows a sharp decline in the *Pinus* curve, a decrease in the diversity of aquatic species and the disappearance of several taxa linked to the presence of a freshwater lagoon (Fig. 7).

This *Pinus* detriment (Fig. 6) 958-901 cal BP) is contemporary with the expansion towards the south of the Christian Kingdoms, between the captures of Braga by King Afonso II (867 AD) and Coimbra by King Fernando I (1064 AD), which would generate strong instability and the need for large quantities of wood for the war industry. Therefore, there would be an intense use of the previously existing *Pinus* plantations. The changes relating to the wetland vegetation (Fig. 9) represent a decrease in the diversity of aquatic species and the disappearance of species linked to freshwater lagoon environments (*Nymphaea*, *Myriophyllum* or *Alisma*). This reveals a process of loss of free water sheet and the wetland conditions. The disappearance is likely related to anthropogenic action.

During the Late Holocene, sedimentation rates were 0.71, 0.31, 4.51 and 2.34 mm/yr (Fig. 8) the highest value obtained in this study, probably related to increased human action over the landscape. Sedimentation rates in other estuaries are higher (e.g. 22 mm/yr on 3600-3200 cal BP and 6.0 mm/yr from 3200 cal BP onwards for the Sado and 1.9 mm/yr for the Tagus in the last 3500 cal BP; in Costa et al., 2019).

NAV4 and NAV5 (Figs. 1 and 9) are located in the border of an incised depression that may correspond to the medieval Fam inlet cited by Felgueiras (2010). Fam, at least until the 14th century, was an important site related to salt exploitation (Abreu, 1988), which is compatible with the Medieval Climatic Optimum.

At least until the 14th century, the importance of Fão was connected to salt exploitation. This is cited in documents from the years AD 959 (*in salinense salinas* in villa Fano), 1059 (*villa cum Salinas*), 1111 (Sé de Braga and the monasteries of Guimarães and Bouro with interests in the *salinas*), and 1153 (salt tax paid to the king). Fisheries (ocean and fluvial) were also considered in the *Inquirições* of 1258 (Abreu, 1988).

In the 14th century, the toll council (*foral da portagem*) of Lisbon referred to Fão as one of the five harbours north of the Douro river, which means that it still had a connection to the sea. According to a toll document of D. Fernando (14th cent), Fão (an urban settlement at the time) had a harbour, probably for fishing boats. Fão was an important fishery harbour from the 12th century (*pescaria de Fão,* Felgueiras, 2010).

5.3.4. Medieval (post-14th century)

During the mid 16th century, its decline had begun due largely to river silting and inlet closing (Felgueiras, 2010), a consequence of LIA in this area (Granja, 1999).

Esposende (still a *lugar* at the time) gained importance from the 14th century and Fão declined. In 1412, king D. João I gave privileges to whomever wanted to live in Fão, which reflects site abandonment. In 1552, Fão would only have two boats while Fam was still represented as a port on Diogo Homem's (1558) map (however, this map may not have depicted up-to-date information). In fact, on Fernão Álvares Secco's map (1580–85) the Cávado mouth had already been mentioned without navigational interest. The same happens with the maps of Waghenaer (1580) and João Teixeira (1648) (Abreu, 1988). Fão's decline would be connected to the beginning of river silting and inlet closing.

Topmost U2 of NAV5 comprises an alternation of median and fine sands moderately well sorted. NAV4 in its U4 presents an alternation of median and coarse sands moderately sorted. These units present a decrease of energy relative to the previous ones (Fig. 10). These sands probably come from the sea (Figs. 3 and 4). The top could correspond to the sands covering lands and houses and the silting of the river and the Fam inlet as referred to in historical texts (e.g. Abreu, 1988; Neiva, 1991; Felgueiras, 2010).

In the second half of the 16th century, with the Cávado silting worsening, a quay was built to block the river drifting to the North. It was later destroyed by the sea as described in the report of Priest Manuel Velho da Costa of 1758 (Losa, 1983). Similarly, all lands on Apúlia were covered by sands in 1586 (Neiva, 1991).

In 1579, the people of Esposende requested of the king (chancellery of D. Sebastião, 1554–1578) the closure of the channels that existed in the river south of the inlet and its repair to prevent the numerous shipwrecks (Felgueiras, 2010, 2018). The charter for intervention works on the quay and the artificial inlet was ordered by the Cardinal-King D. Henrique in 1579.

In 1634, during the chancellery of Filipe III, the people of Fão fought against the "silting with sands coming from the beach". The Fão inlet would already have been closed due to sands. The mother church, near the inlet, pounded by the sea, was under serious threat. The place-name "cangosta dos godos" (meaning narrow and long patch paved with gravel), located near that church (Fig. 1 C), may indicate that this area was once part of a gravel bank of the Fão inlet (or the remains of saltpan floors). This would reinforce the existence of an inlet in this area, a thesis defended by Felgueiras (2010).

This situation would have remained during the 18th century, as merchants wrote to Marquês de Pombal about the deterioration of trade due to inlet obstruction provoked by sands. Another letter from the Arquivo Histórico Ultramarino of 1784 (Felgueiras, 2020) pointed to the decay of Fão due to the great width of the river and sand invasion that almost buried the roof of the church. They request works in order to improve the inlet. In 1774, José Champalimaud de Nussane presented a project for the improvement of the harbour, but it was never realised (Felgueiras, 2020).

From this time onwards, the Cávado lower reach and inlet positions would have moved northwards (probably as happened with the Douro

estuary), where it is presently located. At the beginning of the 20th century, Esposende, on the right river bank, was a *set of mires and swamps devastated by cattle* (Viana, 1928), which means that a wetland (Soares de Carvalho and Granja, 2003) was still present at the time.

The silting of the Cávado estuary and the new inlet continues to date, in the absence of improvement works such as those proposed in the projects of Champalimaud de Nussane and Vilas Boas (Felgueiras, 2020), while the sand spit thins and migrates inland.

6. Conclusions

Multiproxy analyses obtained from three boreholes combined with historical/archaeological and geomorphological data and previous information were the basis for the assessment of sedimentation processes and the environmental evolution of the Cávado palaeoestuary during the Holocene.

The Early Holocene corresponds to a general increase of energy related to river infill with reworked former fluvial/marine sediments and mud coming from soil erosion, under warm and wet conditions and sea level rise. Two levels of finer sediments, one before 9963 cal BP and the other after 9680 cal BP may correspond to drier periods. Fluvial dynamics was much more energetic westwards at Bonança, exposed at the border of a channel, than eastwards in a more sheltered area. The sedimentation rate in this period was 0.36 mm/yr, considerably lower than in other Portuguese estuaries.

Between 6945 and 4064 cal BP, the existence of a peat characterizes very quiet conditions on plains. On the top of the peat (NAV1) some thin layers of poorly sorted sands correspond to events of increased fluvial dynamics, perhaps related to floods. The pollen data reflect the predominance of deciduous forests in the landscape and a very scarce presence of *Pinus*.

During the Late Holocene, a high energetic event, a sudden marine flooding, took place over the upper marsh (peat) somewhere between 4159-4064 cal BP and 3277-3148 cal BP. At the same period, pollen data reveal an intensification in land use and the expansion of agriculture and settlement. The data also shows the loss of water supply or the desiccation of the wetland due to anthropic action. From 3000 cal BP up to the 5th century AD, the Cávado river had a stable connection to the sea. During Augustus' time, the Cávado river was an important Roman anchor point, and salt exploitation in the estuary (especially in Fam) was at its apogee. Regarding these, the expansion of *Pinus* corresponds to forest plantations of local *Pinus* plantations linked to shipbuilding and repair in a port. These plantations, that begin in the final phase of the Roman conquest or during the Suevian Kingdom of Gallaecia, correspond to the oldest pollinic evidence of forest crops in the Iberian Peninsula. The former active channel (Fam inlet, NAV4 and NAV5) was active at least until the 14th century. But during the mid 16th century, its decline had begun due to river silting and inlet closing with sands coming from the sea, as a consequence of LIA. From this time onwards, the Cávado lower reach and inlet position would have moved northwards, where it is presently located. During the Late Holocene, sedimentation rates were 0.71, 0.31, 4.51 and 2.34 mm/yr, the highest value obtained in this study, probably related to increased human action over the landscape during Roman occupation.

Author contributions

Helena Granja (geologist): conceptualization, investigation, writing, validation. Luis Gómez-Orellana (botanist, palynology) conceptualization, investigation, writing. Ana Luísa Costa (geologist): investigation, data curation, visualization. Rui Morais (archaeologist): conceptualization, investigation, writing. César Oliveira (chemist): investigation, editing and review. Pablo Ramil-Rego (botanist, palynology): conceptualization, investigation, writing. José Luís Pinho (engineer): visualization, data curation.

Data availability

The data that support the findings of this study are freely available from the corresponding author, upon reasonable request.

Declaration of competing interest

The authors declare that they have no known competing financial interests or personal relationships that could have appeared to influence the work reported in this paper.

Acknowledgements

This research was partially supported by national funds through the FCT -Foundation for Science and Technology within the scope of UIDB/04423/2020 and UIDP/04423/2020.

The authors would like to acknowledge José Felgueiras for his constant availability and discussion of historical texts and Jean Favennec for some useful suggestions. We would like to acknowledge Luís Gonçalves who did the GPR work in NAVANCOR (PTDC/EPH-ARQ/5204/2012), a project financed by FCT. We would also like to acknowledge Verity Marques for copyediting our paper for submission. We thank Qingzhen Hao, Heike Schneider and two anonymous referees for useful criticism and helpful comments on the manuscript.

References

Abreu, A.A., 1988. O arquivo e as origens da Santa Casa da Misericórdia de Fão. Santa Casa da Misericórdia de Fão, Esposende, p. 254.

Allevato, E., Russo Ermolli, E., di Pasquale, G., 2009. Woodland exploitation and Roman shipbuilding. Méditerranée 112, 33–42.

Almeida, C.A.B., 2005. A exploração do sal na costa portuguesa a norte do Rio Ave. Da Antiguidade Clássica à Baixa Idade Média. In: Amorin, I. (Ed.), Proceedings of the First International Seminar on Portuguese Salt. University of Porto, Porto, pp. 137–170.

Almeida, C.A.B., 2006. O Castro de S. Lourenço, Vila Chã (Esposende). In: Proceedings of Castrenor: Cultura Castrexa no Noroeste Peninsular. Mondariz, Xunta de Galicia, pp. 67–93.

Almeida, C.A.B., Cunha, R.M., 1997. O Castro de S. Lourenço. Câmara Municipal de Esposende Serviços de Arqueologia, Esposende, p. 43.

Baeteman, C., 1999. The Holocene depositional history of the Ijzer palaeo-valley (Western Belgian coastal plain) with reference to the factors controlling the formation of intercalated peat beds. Geol. Belg. 2, 39–72.

Bond, G., Showers, W., Cheseby, M., Lotti, R., Almasi, P., De Menocal, P., Priore, P., Cullen, H., Hajdas, I., Bonami, G., 1997. A pervasive millennial-scale cycle in North Atlantic Holocene and glacial climates. Science 278, 1257–1266.

Boski, T., Camacho, S., Moura, D., Fletcher, W., Wilamowski, A., Veiga-Pires, C., Correia, V., Loureiro, C., Santana, P., 2008. Chronology of the sedimentary processes during the postglacial sea level rise in two estuaries of Algarve coast, Southern Portugal. Estuar. Coast Shelf Sci. 77, 230–244.

Cabral, J.M., 1993. Neotectónica de Portugal Continental. PhD thesis. University of Lisbon, Lisbon, p. 435.

Costa, A.M., Freitas, M.C., Leira, M., Costas, S., Costa, P.J.M., Andrade, C., Bao, R., Duarte, J., Rodrigues, A., Cachão, M., Araújo, A.C., Diniz, M., Arias, P., 2019. The role of climate, marine influence and sedimentation rates in late-Holocene estuarine evolution (SW Portugal). Holocene 29, 622–632.

Dias, J.M.A., Boski, T., Rodrigues, A., Magalhães, F., 2000. Coast line evolution in Portugal since the Last Glacial Maximum until present - a synthesis. Mar. Geol. 170, 177–186.

Felgueiras, J.E.S., 2010. Sete Séculos no mar (XIV a XX). Notícia histórica dos Estaleiros de Esposende e Fão, vol. 3. Centro Marítimo de Esposende/Forum Esposendense, Esposende.

Felgueiras, J.E.S., 2018. Naufrágios na costa de Esposende. Mar do Senhor. Naufrágios, acidentes e incidentes nos rios e na costa. Chiado Editora, Esposende, p. 468.

Felgueiras, J.E.S., 2020. Francisco António de Faria, o Eng. Vilas Boas e o encanamento do Cávado. Boletim Cultural de Esposende 1 (3rd series), 73–133.

Folk, R.L., 1954. The distinction between grain size and mineral composition in sedimentary-rock nomenclature. J. Geol. 62 (4), 344–359. http://www.jstor.org/stable/30065016.

Folk, R.L., Ward, W.C., 1957. Brazos river bar: a study in the significance of grain size parameters. J. Sediment. Petrol. 27, 3–26.

Friedman, G.M., 1967. Dymanic processes and statistical parameters compared for size frequency distribution of beach and river sands. J. Sediment. Petrol. 37, 327–354.

Friedman, G.M., 1979. Differences in size distributions of populations of particle among sands of various origins. Sedimentology 26, 859–862.

Gomes, S.D., Fletcher, W.J., Rodrigues, T., Stone, A., Abrantes, F., Naughton, F., 2020. Time-transgressive Holocene maximum of temperate and Mediterranean forest

development across the Iberian Peninsula reflects orbital forcing. Palaeogeogr. Palaeoclimatol. Palaeoecol. 550, 109739.
Gómez-Orellana, L., Ramil-Rego, P., Martínez-Sánchez, S., 2001. Landscape modifications during the upper pleistocene-holocene in the NW atlantic margin of iberian peninsula. Estud. do Quat. 4, 79–96.
Gómez-Orellana, L., Ramil-Rego, P., Muñoz-Sobrino, C., Bettencourt, A., 2010. El paisaje Holoceno en la Serra de Arga (NW Portugal). In: Bettencourt, A., Alves, M.I.C., Monteiro-Rodrigues, S. (Eds.), Variações Paleoambientais e Evolução Antrópica no Quaternário do Ocidente Peninsular, pp. 53–60. Braga.
Gómez-Orellana, L., Ramil-Rego, P., Ferreiro da Costa, J., Muñoz Sobrino, C., 2021. Holocene environmental change on the Atlantic coast of NW Iberia as inferred from the Ponzos wetland sequence. Boreas. https://doi.org/10.1111/bor.12535.
González-Villanueva, R., Pérez-Arlucea, M., Costas, S., Bao, R., Otero, X.L., Goble, R., 2015. 8000 years of environmental evolution of barrier-lagoon systems emplaced in coastal embayments (NW Iberia). Holocene 25, 1786–1801.
Granja, H.M., 1999. Evidence for Late Pleistocene and Holocene sea-level, neotectonic and climatic indicators in northwest coastal zone of Portugal. Neth. J. Geosci. 77, 233–245.
Granja, H.M., 2013. Late Holocene palaeonvironmental reconstitution. In: Morais, R., Granja, H., Cerdán, A. (Eds.), O irado mar atlântico. O naufrágio bético augustano de Esposende (Norte de Portugal), pp. 221–235. Braga.
Granja, H.M., Morais, R., 2012. Was There a Roman Shipwreck at Marinhas (Esposende, NW Portugal)? 4th International Geologica Belgica Meeting, Bruxels, Belgium, p. 1.
Granja, H.M., Rocha, F., Matias, M., Moura, R., Caldas, F., Marques, J., Tareco, H., 2010. Lagoa da Apúlia: a residual lagoon from Late Holocene (NW coastal zone of Portugal). Quat. Int. 221, 46–57.
Granja, H.M., Monteiro-Rodrigues, S., Danielsen, D., 2016. Changing environments and human settlement during mid-holocene in Rio de Moinhos beach (Esposende, Northern Portugal). Estud. do Quat. 14, 25–40.
Grimm, E.C., 1990. TILIA and TILIAGRAPH: PC spreadsheets and graphics software for pollen data. INQUA Working Group on Data Handling Methods, Newslett 4, 5–7, 2015.
Henriques, R.F., 2004. SEDMAC/SEDPC: an application to support particle size analysis of unconsolidated sediments. Proc. 32nd Int. Geol. Congr. Flor. 20–28, 726.
Hoffman, G., 1989. Estratigrafia Holocénica da linha da costa nos vales dos Rios Sizandro (Portugal) e Guadiana (Portugal e Espanha). Geolis 3 (1/2), 137–143.
Leorri, E., Fatela, F., Drago, T., Bradley, S.L., Moreno, J., Cearreta, A., 2012. Lateglacial and Holocene coastal evolution in the Minho estuary (N Portugal): implications for understanding sea-level changes in Atlantic Iberia. Holocene 23, 353–363.
Losa, A., 1983. Terras de Esposende em 1758 (segundo os manuscritos da Torre do Tombo), prefácio e notas. Boletim Cultural de Esposende 3, 67–75.
Mateus, J.E., 1992. Holocene and Present-Day Ecosystems of the Carvalhal Region, Southwest Portugal. PhD Thesis. University of Utrecht, p. 184.
Mayevsky, P.A., Rohling, E.E., Stager, J.C., Karlén, W., Maasch, K.A., Meeker, L.D., Meyerson, E.A., Gasse, F., van Kreveld, S., Holmgren, K., Lee-Thorp, J., Rosqvist, G., Rack, F., Staubwasser, M., Schneider, R., Steig, E.J., 2004. Holocene climate variability. Quat. Res. 62, 243–255.
Moore, P.D., Webb, J.A., Collinson, M.E., 1991. Pollen Analysis. Blackwell Scientific Publications, p. 217.
Morais, R., 2005. Autarcia e Comércio em Bracara Augusta. Contributo para o estudo económico da cidade no período Alto-Imperial, Bracara Augusta, vol. 2. Escavações Arqueológicas, Braga, p. 957.
Morais, R., 2013. Um naufrágio bético, datado da época de Augusto, em Rio de Moinhos (Esposende, Norte de Portugal). In: Morais, R., Granja, H., Cerdán, A. (Eds.), O irado mar atlântico. O naufrágio bético augustano de Esposende (Norte de Portugal), pp. 309–334. Braga.
Morais, R., 2020. Naufrágio bético e provável embarcadouro de época romana em Rio de Moinhos (Esposende, Norte de Portugal). Boletim Cultural de Esposende, pp. 203–215.
Muñoz-Sobrino, C., Ramil-Rego, P., Gómez-Orellana, L., Díaz-Varela, R.A., 2005. Palynological data on major Holocene climatic events in NW Iberia. Boreas 34, 381–400.
Naughton, F., Sanchéz Goñi, M.F., Drago, T., Freitas, M.C., Oliveira, A., 2007. Holocene changes in the Douro estuary (northwestern Iberia). J. Coast Res. 23, 711–720.
Naveiro López, J.L., 1991. El comercio antiguo en el NW peninsular. Lectura Histórica del Registo Arqueológico. Monografías Urxentes do Museu, Museu Arqueolóxico, A Coruña, p. 276.
Neiva, M.A.P., 1991. In: Esposende: páginas de memórias, personal edition, p. 244. Esposende.
Oliveira, C., Kuźniarska-Biernacka, I., Parpot, P., Neves, I.C., Fonseca, A.M., Morais, R., 2013. Chemical analysis of organic residues in anphorae from the Baetica shipwreck of Esposende. In: Morais, R., Granja, H., Cerdán, A. (Eds.), O irado mar atlântico. O naufrágio bético augustano de Esposende (Norte de Portugal), pp. 263–281. Braga.
Oliveira, C., Morais, R., Araújo, A., 2015. Application of gas chromatography coupled with mass spectrometry to the analysis of ceramic containers of Roman period - evidence from the peninsular northwest. In: Oliveira, C., Morais, R., Cerdán, A. (Eds.), ArchaeoAnalytics: Chromatography and DNA Analysis in Archaeology, Esposende City Council, Esposende, pp. 193–212.
Pritchard, D.W., 1952. Estuarine hydrography. In: Landsberg, H.E. (Ed.), Advances in Geophysics 1. Academic Press, New York, pp. 243–280.
Ramil-Rego, P., 1992. La vegetación cuaternaria de las Sierras Septentrionales de Lugo a través del análisis polínico. Tesis Doctoral. Facultad de Biología. Universidad de Santiago de Compostela, p. 456.
Ramil-Rego, P., Gómez-Orellana, L., 2016. Clima, paisaxe e acción humanana no Noroeste da Peninsula Ibérica durante a ldade do Ferro e a Romanización: mitos e realidades. In: Dolores Dopico Caínzos, M., Villanueva Acuña, M. (Eds.), Clausus est Ianus, PHILTÁTE 1: Studia et acta antiquae Callaeciae. Servizo de Publicacións da Deputación de Lugo, Lugo, pp. 163–183.
Ramil-Rego, P., Taboada Castro, M.T., Díaz-Fierros, F., Aira Rodríguez, M.J., 1996. Modificación de la cubierta vegetal y acción antrópica en la región del Minho (Norte de Portugal) durante el Holoceno. In: Ramil-Rego, P., Fernández Rodríguez, C., Rodríguez Guitián, M. (Eds.), Biogeografía Pleistocena de la Península Ibérica, Xunta de Galicia, Santiago de Compostela, pp. 199–214.
Ramil-Rego, P., Muñoz Sobrino, C., Rodríguez Guitián, M., Gómez-Orellana, L., 1998. Differences in the vegetation of the north iberian peninsula during the last 16,000 years. Plant Ecol. 138, 41–62.
Ramil-Rego, P., Gómez-Orellana, L., Fernández, B.N., Muñoz-Sobrino, C., García-Gil, S., 2009. Cambio climático y dinámica del paisaje en Galicia. Recursos Rurais 5, 21–47.
Ramil-Rego, P., Meireles, J., Gómez-Orellana, L., Muñoz-Sobrino, C., 2015. Evolución del paisaje y acción humana en el noroeste de Portugal durante el Holoceno. Férvedes 8, 65–74.
Ramos-Pereira, A., Ramos, C., Danielsen, R., Trindade, J., Soares, A.M., Granja, H., Martins, J.M.M., Portela, P.J.C., Torres, A., Araújo-Gomes, J., 2019. Late Holocene natural and man induced environmental changes in the Western Iberian coast: assessing forcing factors. In: Ramos-Pereira, A., Leal, M., Bergonse, R., Trindade, J., Reis, E. (Eds.), Água e Território – um tributo a Catarina Ramos. Centro de Estudos Geográficos, University of Lisbon, Lisbon, pp. 217–249.
Rasmussen, S.O., Bigler, M., Blockley, S.P., Blunier, T., Buchardt, S.L., Clausen, H.B., Cvijanovic, I., Dahl-Jensen, D., Johnsen, S.J., Fischer, H., Gkinis, V., Guillevic, M., Hoek, W.Z., Lowe, J.J., Pedro, J.B., Popp, T., Seierstad, I.K., Steffensen, J.P., Svensson, A.M., Vallelonga, P., Vinther, B.M., Walker, M.J., Wheatley, J.J., Winstrup, M., 2014. A stratigraphic framework for abrupt climatic changes during the Last Glacial period based on three synchronized Greenland ice-core records: refining and extending the INTIMATE event stratigraphy. Quat. Sci. Rev. 106, 14e28.
Ribeiro, I., Granja, H., 2000. Holocene evolution: evidences for sea-level changes in the coastal sectors of Marinhas and Belinho (Esposende). In: 3rd Symposium on the Iberian Atlantic Margin. Faro, Portugal, pp. 123–124.
Rodrigues, A., Magalhães, F., Alveirinho Dias, J., 1991. Evolution of the north Portuguese coast in the last 18 000 years. Quat. Int. 9, 67–74.
Soares de Carvalho, G., Granja, H., 2003. As mudanças da zona costeira pela interpretação dos sedimentos plistocénicos e holocénicos (a metodologia aplicada na zona costeira do NO de Portugal). Revista da Faculdade de Letras - Geografia XIX, pp. 225–236.
Solomina, O.N., Bradley, R.S., Hodgson, D.A., Ivy-Ochs, S., Jomelli, V., Mackintosh, A.N., Nesje, A., Owen, L.A., Wanner, H., Wiles, G.C., Young, N.E., 2015. Holocene glacier fluctuations. Quat. Sci. Rev. 111, 9–34.
Sousa, C., Boski, T., Pereira, L., 2018. Holocene evolution of a barrier island system. Ria Formosa, South Portugal, The Holocene 29, 64–76.
Stuiver, M., Reimer, P.J., Reimer, R.W., 2021. CALIB 8.2 [WWW program] at. http://calib.org. (Accessed 22 December 2021).
Teixeira, C., Medeiros, A.C., Alves, C.A.M., Moreira, M.M., 1969. Carta Geológica de Portugal na escala 1:50 000. Notícia Explicativa da Folha 5-C, Barcelos. Serviços Geológicos de Portugal, Lisbon.
Tucker, M.E., 1988. Techniques in Sedimentology. Blackwell Scientific Publications, p. 408.
Viana, X., 1928. Almanaque de Espozende 1928. Tipografia Vieira, Esposende.
Wang, T., Surge, D., Mithen, S., 2012. Seasonal temperature variability of the Neoglacial (3300-2500 BP) and Roman Warm Period (2500-1600 BP) reconstructed from oxygen isotope ratios of limpet shells (*Patella vulgata*), Northwest Scotland, Palaeogeogr. Palaeoclimatol. Palaeoecol. 317–318, 104–113.
Wanner, H., Beer, J., Butikofer, J., Crowley, T.J., Cubasch, U., Fluchiger, J., Goosse, H., Grosjean, M., Joos, F., Kaplan, J.O., Kuttel, M., Muller, S.A., Prentice, I.C., Solomina, O., Stocker, T.F., Tarasov, P., Wagner, M., Widmann, M., 2008. Mid- to Late Holocene climate change: an overview. Quat. Sci. Rev. 27, 1791–1828.
Zalat, A., Welc, F., Nitychoruk, J., Marks, L., Chodyka, M., Zbucki, L., 2018. Last two millennia water level changes of the Mlynek lake (northern Poland) inferred from diatoms. Stud. Quat. 35 (2), 77–89.